


Research Article

Exploration of Tunnel Lining Falling Block Remediation Using Polyurea Material

Changyu Yang,¹ Xun Yuan ,¹ Fang Wang,¹ Yong Zhu,¹ Ang Chen,¹ Jieyuan Zheng,¹ Yi Yang,² Hui Wang,³ and Jijun Guo³

¹China Railway Eryuan Engineering Group Co. Ltd., Chengdu 610031, China

²China Railway Chengdu Group Co. Ltd., Chengdu 610081, China

³Chongqing Construction Headquarters of China Railway Chengdu Group Co. Ltd., Chongqing 400000, China

Correspondence should be addressed to Xun Yuan; yuanxun3@ey.crec.cn

Received 27 September 2022; Revised 28 October 2022; Accepted 24 November 2022; Published 17 May 2023

Academic Editor: Fuqiang Ren

Copyright © 2023 Changyu Yang et al. This is an open access article distributed under the Creative Commons Attribution License, which permits unrestricted use, distribution, and reproduction in any medium, provided the original work is properly cited.

Tunnel lining falling blocks can cause great threats to traffic safety, resulting in traffic interruptions or speed limits and endangering operational safety. Traditional lining disease remediation measures have low efficiency and high costs and are time consuming. Combining the research methods used in the literature, indoor testing, and model experiments, a very normal material, namely, polyurea spray film material, is proposed as a means by which to remediate the lining falling block disease in tunnels. A 1:1 tunnel lining structure model was established at the site, and four experimental conditions were tested. The experiments revealed that the tensile stress was less than the tensile strength and that no tensile fracture occurred in the polyurea spray film material under the joint action of the block's self-weight and aerodynamic loads. Factors such as side seam treatment, surface sanding, and spray temperature may influence the bond strength of the polyurea spray film material. In order to remediate the issue of lining blocks falling, we recommended increasing the bond strength between the spray film material and the concrete or increasing the thickness of the polyurea spray film material.

1. Introduction

By the end of 2020, China's railway operating mileage reached 145,000 km. A total of 16,798 railway tunnels have been put into operation, with a total length of about 19,630 km. The total length of the high-speed railways that have been put into operation is about 37,000 km, and the total number of tunnels is 3,631, with a total length of about 6,003 km, as shown in Table 1 [1].

The railways have a wide distribution range, a high proportion of tunnels, and complex geological and hydrological conditions [2]. Tunnel lining with high reliability is the key to ensuring the safety of high-speed railways. In recent years, most of the new operating railways have been high-density and high-speed electrified trunk and passenger-dedicated railways [3]. Tunnel lining that contain falling blocks can cause great threats to traffic safety, resulting in traffic interruptions or speed limits, endangering operational safety [4].

In the construction process, under-excavation control, the installation of subwindows into the mold, centralized vibrating, mold grouting, equipment modifications, and construction method improvements are carried out [5]. However, tunnel vault lining back voids, crack leakage, block drops, and other issues continue to appear, threatening the safety of railway traffic seriously [6].

Due to the influence of hydrogeological conditions, terrain, climate, natural disasters, and various unfavorable factors in the design, construction, operation, and management of tunnels can face various issues after being put into use, such as lining cracks and block drops [7]. These issues shorten the maintenance cycle and service life of the tunnel and seriously threaten the safety of traffic and pedestrians in the tunnel [8]. In recent years, safety accidents caused by tunnel diseases have abounded. In 1999, there were three lining block accidents in Japanese railway tunnels [9]. In July 2006, a tunnel in the Boston Central Tunnel Project collapsed

TABLE 1: Statistical table of China's high-speed rail tunnel profile.

High-speed rail status	Tunnel number	Tunnel cumulative length (km)
Under operation	3671	6003
Under construction	1811	2750
Planning	3525	7966

on top of a concrete slab [10]. Once a falling block accident occurs in an operational tunnel, the consequences are often very serious; this has attracted the attention of the transportation departments and tunnel engineering and technical personnel of various countries [11]. They have carried out inspections and treatments of tunnel diseases. Since the concrete block drop accident in the tunnels in Fukuoka Prefecture in June 1999, the Japan Transport Ministry has required the inspection of 3,360 km of tunnels among the 4,826 tunnels that are part of the national railway line [12]. Most of the tunnels in Italy were built in the 1960s, and inspections revealed that a large number had varying degrees of lump-dropping disease due to aging, load variability, environmental influences, and other influences [13].

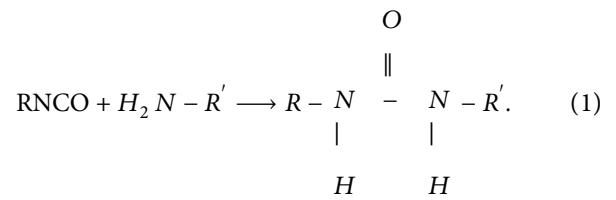
At present, lining disease remediation measures include adding bushings, the integral removal of arches, partial dismantling, polymer repair mortar filling, corrugated plate reinforcement, carbon fiber cloth reinforcement, steel belt plus anchor reinforcement, and lining inner grouting [14]. The existing measures are commonly applied, and the technologies are relatively mature. However, for the operation of tunnels, disease remediation can only be carried out using skylight time. By deducting the inspection time both inside and outside of the tunnel, the actual construction time of each skylight was found to be only a few hours [15]. The construction process, such as cast-in-place concrete or polymer mortar, is complex, the labor operation intensity is large, and the survival speed is slow, resulting in the existing remediation measures having low efficiency and high costs [16].

In view of the skylight operation time being short, time-consuming, inefficient, and with high remediation costs and other issues for existing lining disease remediation, a polymer spray film reinforcement material, namely, polyurea, is proposed in this paper. Tunnel lining disease can be rectified through surface spraying and other means. At present, there is little use of polyurea in railway engineering. It is mostly used for bridge deck waterproofing. This study combines the working environment and disease remediation requirements of tunnel lining and adopts the research methods used in the literature, such as indoor testing and model testing, to study the material performance indicators, construction process, mechanical equipment configuration, acceptance standards, construction efficiency, and economic efficiency. Finally, a complete set of spray film reinforcement technologies and construction methods for lining disease remediation are formed.

2. Application Status of Polyurea Spray Film Materials

2.1. Function Mechanism. Polyurea materials are polymers based on the chemical reaction of isocyanates, which are

generated by the reaction of isocyanates with amino compounds [17]. The reaction of isocyanate with amines is part of the gradual addition and polymerization of hydrogen transfer, which is caused by the nucleophilic center of the amine attacking the positive carbon ions of the isocyanate group [18]. The hydrogen atoms in the active hydrogen compound are transferred to the N atoms in the -NCO group, and the remaining groups and carbonyl C atoms are combined to form a urea group, the essence of which is the reaction of the semi-prepolymer with the amino polyether and amine chain extender [19]. Due to the high activity of amino polyether and the alkalinity of the N atom, the reaction does not require a catalyst and can be cured and formed in a very short time. The reaction process is shown in the following formula (1):



The formation principle of spray film is impact mixing. The A and R component liquids with high reactivity collide with each other under a high-pressure drive. The liquids are mixed by turbulence in the gun body mixing room, atomized by the spray gun, and then mixed evenly and sprayed on the substrate surface in a very short application period. Finally, an overall seamless polyurea elastomer spray layer is formed [20].

Coating adhesion strength refers to the degree of firmness of the coating film and the surface of the substrate, which are bound together by physical and chemical forces [21]. The intensity of the adhesion strength depends on the number of the polymer polar groups and the polar groups on the surface of the substrate in the coating, as well as their interaction, which is mainly determined by chemical bonds, intermolecular forces, and mechanical forces [22]. The essence of adhesion is an interfacial force, including the cohesion of the coating itself and the adhesion of the coating film to the substrate, as well as the internal stress after the coating is formed [23]. Together, these three factors affect the adhesion of the coating to the substrate. Coating cohesion is the characteristic of the coating itself. The adhesion is generated by the physicochemical action of the coating and the substrate [24]. The stress on the coating comes from two aspects: one is caused by external forces, and the other is generated when the film is formed. Therefore, the adhesion of the coating to the substrate is mainly affected by the following two factors:

- (1) The substrate surface treatment, which includes physical and chemical methods. The chemical method is to pickle and then carry out grinding and phosphating. The physical methods include hand sanding, sand blasting, or blasting. Both the physical and chemical methods require close and sufficient contact between the coating substance and the surface

material of the substrate. If there are oil stains, rust, or other substances on the surface of the substrate, these will hinder the close contact between the coating and the surface of the substrate [25]. Therefore, the substrate surface must be treated before coating. In addition, in order to increase the contact area between the coating and the substrate surface, the substrate surface is sand-blasted or shot-blasted to improve the adhesion of the coating to the substrate.

- (2) The spraying temperature. The porosity and fracture rate of the adhesive surface of the coating can have a certain impact on the adhesion of the coating and the corrosion resistance of the coating. Therefore, in the painting process, it is necessary to reduce the porosity of the coating to improve the performance of the coating [26]. Porosity is related to the formulation of the coating on the one hand and the spray temperature on the other hand. The coating process of the paint involves the coexistence of physical and chemical processes. During the coating process, the coating is heated and melted on the substrate while the curing reaction of the epoxy resin occurs. The spraying temperature refers to the temperature of the substrate when the powder is sprayed on the substrate. If the spraying temperature is low, the viscosity of the resin after melting will be high, the gelling time will be long, the curing reaction speed will be slow, the wetting time with the substrate will be long, and the cohesion of the formed coating will be high. On the contrary, if the spraying temperature is high, the resin melt viscosity will be low, the gelling time will be short, the curing reaction speed will be fast, the wetting time with the substrate will be short, and the cohesion of the resulting coating will be low. If considered from the perspective of full wetting of the coating and the substrate, the wetting effect due to low-viscosity and a long wetting time is good. However, low-viscosity and long-term wetting are contradictory in the process of powder coating because the speed of the curing reaction is proportional to the curing temperature. If the spraying temperature is high, the melt viscosity will be low, but the time for cross-linking and curing will be shortened at the same time. It is more important to choose a relatively reasonable temperature in the spraying process. When the shear stress of the coating is greater than the adhesion force of the coating to the substrate, the coating is easily peeled off of the substrate. Increasing the temperature of the coating can improve the movement of the electron cloud, which is conducive to the formation of covalent bonds between the substrate and the coating, thereby improving the adhesion of the coating. However, the porosity of the coating, especially the porosity of the bonded surface, will increase with the increase in the spraying temperature, and the increase in porosity will affect the adhesion of the coating to the substrate [27].

2.2. Prospect of Polyurea Material for Use in Tunnel Falling Block Disease Remediation. The advantages of the polyurea protective coating mainly include excellent mechanical properties, 100% solid content (zero VOC), green environmental protection, convenient spraying construction, seamless overlapping, and an ultra-long service life. Due to these excellent properties, spray polyurea elastomer technology has previously been used in structures such as the Boston Subway Tunnel and offshore drilling platforms. Bo [28] studied the corrosion resistance of anticorrosion coatings in different corrosive environments, and the results showed that the corrosion resistance of polyurea coatings in wet and dry circulation, brine soaking, and wet and hot corrosive environments was far superior to the corrosion resistance of polyurethane coatings and epoxy cloud iron coatings. Lü [29] et al. synthesized a new type of polyaspartic polyurea elastomer with polyaspartic acid grease. Through the study of its accelerated aging, dynamic mechanical behavior, and marine aging behavior, it was concluded that polyaspartic polyurea elastomer has good mechanical properties and corrosion resistance. Liu [30] studied the resistance to chloride ion permeation of polyurea coatings under stress conditions and without stress, and the results showed that spraying polyurea coatings on concrete surfaces can significantly improve chloride ion permeability. Yang [31] studied the acid and alkali resistance and frost resistance of concrete protected by polyurea coating and polyurethane coating, and the results showed that the acid and alkali resistance and frost resistance of polyurea coating were better than those of polyurethane coating. Li et al. [32] studied the application of polyurea in offshore concrete protection, analyzed the influencing factors of adhesion, studied the corrosion resistance of polyurea protection on the Qingdao Bay Bridge, and discussed the frost resistance and chloride ion permeation resistance of coated concrete. Wang [33] studied the effects of substrate strength, maintenance age, primer type, and temperature and humidity on the adhesion of polyurea coatings on concrete substrates.

Based on the excellent properties of polyurea materials, they have been widely used in China, such as in the Beijing Olympic Venues, Qingdao Jiaozhou Bay Cross-Sea Bridge, Beijing-Shanghai High-Speed Railway, and The Immersed Tube Tunnel part of the Hong Kong-Zhuhai-Macao Cross-Sea Bridge. Polyurea has been recognized by an increasing number of people and has been increasingly applied in major projects. Polyurea technology has gradually become one of the most promising materials of this century. According to the existing research and applications, polyurea spray film reinforcement materials are currently mostly used for waterproofing of new projects in the field of underground engineering. They are less frequently used in tunnel disease remediation, and the only cases mainly concern water leakage. There are many types of railway tunnel diseases, and diseases such as hollows and falling blocks are especially important as they endanger driver's safety. There is no research on or application of polyurea spray film materials in this field. From the perspective of improving the efficiency of rectification and reducing the cost of remediation, the

research on the use of spray film reinforcement materials for tunnel lining disease remediation technology is of very important theoretical significance and practical engineering value.

3. Analysis and Assumptions of the Mechanical Properties of Polyurea Materials

3.1. The Main Function of Polyurea Spray Film Material. Regarding spray film reinforcement materials used for tunnel lining disease remediation, the main role of polyurea spray film is to cover the lining block to prevent falling blocks and their threat to the safety of driving.

As shown in Figure 1, on the concrete lining with a thickness of T , there is a circular concrete test block $AA'BB'$ with a diameter of r_1 and a mass of m . At the initial moment, the test block is not separated from the lining and is supported by a polyurea elastomer with a diameter of $r_1 + 2r_2$ and a bond strength of ψ . It can be seen that the protective effect of the spray polyurea elastomer on the separated concrete test block on the lining is essentially the support force provided by the ring polyurea elastomer with width r_2 , while the polyurea elastomer with the diameter of the r_1 part at the bottom of the test block does not provide force. Therefore, the most dangerous points of the entire care system are point A and point A' .

Since the polyurea spray film is a flexible material, the vertical and horizontal directions of the load at point A and point A' do not provide the supporting force that the rigid body does. The support of the test block depends on the adhesion of the spray polyurea elastomer and the dragging force of the film after the spray film is disengaged.

3.2. Loads on the Spray Film Material. Under different test conditions, the spray film material was mainly subjected to tensile pressure and shear effects caused by the self-weight of the arch drop block and the additional aerodynamic effect.

3.2.1. Self-Weight of the Arch Drop Block. When lining block falling occurs, the spray film material must first withstand the gravity applied by the self-weight of the falling block, which is determined by the concrete bulk weight and the size of the test block.

3.2.2. Aerodynamic Loads. When the multiple unit (EMU) passes through a short tunnel, the impact of aerodynamic loads on the pressure change inside the vehicle is small, while the impact on the tunnel structure and its ancillary facilities cannot be ignored. The high-speed passage of the train in the tunnel causes a drastic change in the air pressure inside the tunnel, and the aerodynamic effect generated has a great impact on the spray film material. High-speed trains produce an aerodynamic fatigue load when running in the tunnel. The role of the pneumatic fatigue load is to cause the spray film material and the initial stable small crack on the lining to quickly develop. At the same time, new cracks can also occur around the periphery of the existing cracks. The

new cracks extend towards the weak points in the material and connect with the existing cracks, causing macroscopic damage to the material.

3.3. Stress Model Assumptions. The antifall block of lining in this study refers to the loosening area of the lining locally. Under the premise of not affecting the overall stability of the lining structure, the spray film material is used to achieve the purpose of creating an antifall block. Focusing on the tensile strength of the spray film and the bonding strength between it and the concrete, the calculation ignores the friction between the test block and the lining wall.

3.3.1. Calculation of the Spray Film Material Force of the Circular Concrete Test Block

(1) Spray Film Bond Strength When Only the Self-Weight of the Test Block is Considered. The bonding strength and tensile strength of the spray film material to the lining concrete surface on the concrete test block at the top of the lining is calculated according to the principle of the minimum circumference of the circular boundary, as shown in Figure 2. Combined with the actual situation of the tunnel section, the diameters of the test block r_1 are 0.5 m, 1 m, 2 m, 3 m, 4 m, 5 m, and 6 m, respectively. The thickness is $T = 0.5$ m, and the concrete bulk weight is $\gamma = 23$ kN/m³. The bond strength of the spray film material ψ is assumed to be outside the boundary of the falling block according to the force area, $L_1 = 0.01$ m. The tensile strength is calculated under the assumption that faulting of the block end is $h_1 = 0.005$ m after spraying, and it is assumed that the material is still within the elastic range at this time.

According to the principle of force balance, in order to prevent the test block from falling, the following conditions must be met:

$$\gamma\pi\frac{r_1^2}{4}T = \pi r_1 L_1 \psi. \quad (2)$$

From this, the calculation formula for the spray film bond stress ψ is as follows:

$$\psi = \frac{\gamma r_1 T}{4L_1}. \quad (3)$$

(2) Bond Strength of the Spray Film When Both the Block Weight and Aerodynamic Loads are Taken into Account. According to the additional pressure recommendation values for auxiliary facilities in tunnels as found in the China high-speed railway design code, the bond strength of the spray film material to the concrete surface is shown in Table 2 under the condition of single and double lines at different speeds.

According to Table 2, the worst operating condition is when trains meet in double lines with a speed of 350 km/h. The bond strength of the sprayed film material to the surface of the lined concrete should be greater than 14.8 kPa

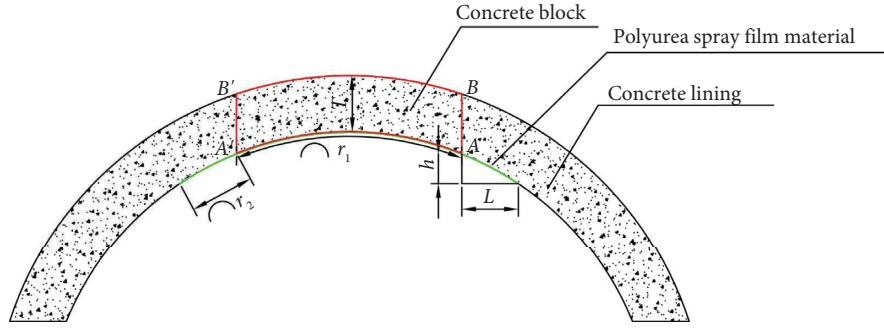


FIGURE 1: Schematic diagram of the calculation of the bearing of the spray polyurea material.

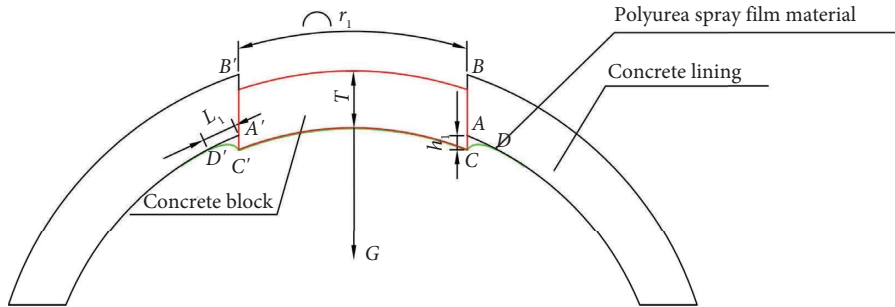


FIGURE 2: Schematic of the calculation when only gravity is considered.

TABLE 2: Additional pressure recommendation values in high-speed rail tunnels.

Nos	Operating condition	Positive peak pressure (kPa)	Passive peak pressure (kPa)	Bond stress requirement (kPa)
1	Single line, 70 m ² , 300 km/h,	2.6	-3.9	>6.4
2	Single line, 70 m ² , 350 km/h	3.4	-5.1	>8.5
3	Double lines, 100 m ² , 300 km/h	1.6	-2.8	>4.4
4	Double lines, 100 m ² , 350 km/h	2.2	-3.5	>5.7
5	Double lines, 100 m ² , 350 km/h, trains meet	5.9	-8.9	>14.8
6	Double lines, 92 m ² , 250 km/h	1.2	-1.8	>3.0
7	Double lines, 92 m ² , 250 km/h, trains meet	3.5	-5.4	>8.9
8	Single line, 58 m ² , 250 km/h	2.2	-3.3	>5.5

(0.0148 MPa). Therefore, the aerodynamic loads on the test block under the most unfavorable operating conditions can be calculated as follows:

$$P = 14.8\pi \frac{r_1^2}{4}. \quad (4)$$

A schematic diagram for the calculation of the bond strength of the spray film material, taking into account both the self-weight of the test block and the aerodynamic load, is shown in Figure 3.

Combining equations (3) and (4) with Figure 3, the spray film bond stress calculation formula under this condition is as follows:

$$\psi = \frac{(\gamma T + 14.8)r_1}{4L_1}. \quad (5)$$

(3) *Tensile Strength of the Spray Film When Both the Block Weight and Aerodynamic Loads are Taken into Account.* The

tensile strength ξ of the spray film is calculated according to Figure 4. When the test block falls, it is caught by the drag action of the spray film. The component of the spray film tension in the vertical direction is canceled out by the gravity and aerodynamic load of the test block, and the components of the ring spray film tension in the horizontal direction cancel each other out. The entire care system reaches a balanced state.

Width of the torn spray film can be calculated as follows:

$$l = \sqrt{L_1^2 + h_1^2}. \quad (6)$$

Angle between spray film and test block can be calculated as follows:

$$\theta = \arctan \frac{L_1}{h_1}. \quad (7)$$

The component of the spray film tension in the vertical direction can be calculated as follows:

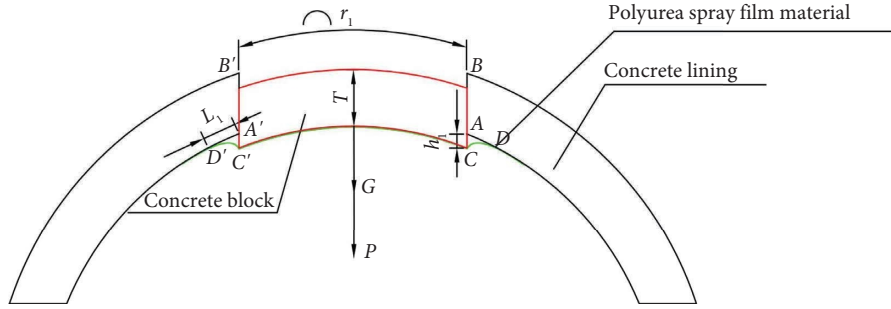


FIGURE 3: Schematic diagram of the calculation of bond stress taking into account both gravity and aerodynamic loads.

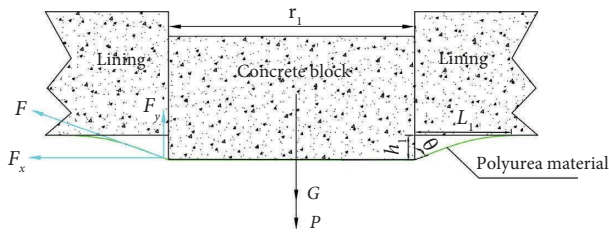


FIGURE 4: Calculation schematic diagram of spray film tensile stress.

$$F_y = F \cos \theta. \quad (8)$$

Spray film tension can be calculated as follows:

$$F = \pi r_1 l \xi. \quad (9)$$

Combining formula (2) and (4) and formula (6)~(9), the tensile stress ξ of the spray film can be obtained as follows:

$$\xi = \frac{(T\gamma + 14.8)r_1}{4\sqrt{L_1^2 + h_1^2} \cos \arctan L_1/h_1}. \quad (10)$$

(4) *Tensile Strength of the Spray Film When Only the Self-Weight of the Test Block Is Considered.* When only the self-weight of the falling test block is considered, without consideration of the aerodynamic load, the schematic diagram of the force of the spray film support system is shown in Figure 5.

According to equation (10) and Figure 5, the tensile stress of the spray film at this time is calculated as follows:

$$\xi = \frac{T\gamma r_1}{4\sqrt{L_1^2 + h_1^2} \cos \arctan L_1/h_1}. \quad (11)$$

3.3.2. *Calculation of the Spray Film Material Force of the Rectangular Concrete Test Block.* According to the calculation result of the circular falling block, the force condition of the spray film material under the rectangular falling block can also be obtained.

(1) *Spray Film Bond Strength When Only the Self-Weight of the Test Block is Considered.* As can be seen from Figure 2, when the concrete test block is r_1 long and r_2 wide, equation (2) can be converted to

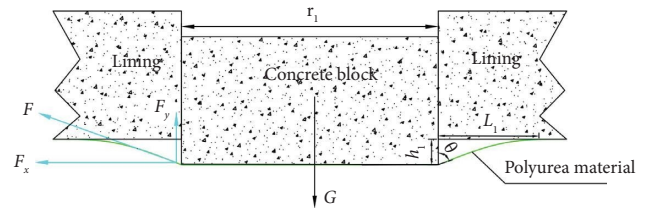


FIGURE 5: Calculation schematic diagram of spray film tensile stress when subjected to gravity alone.

$$\gamma r_1 r_2 T = [(2L_1 + r_1)(2L_1 + r_2) - r_1 r_2] \psi. \quad (12)$$

From this, it is possible to obtain the formula for calculating the bonding stress of the spray film material when considering only the self-weight of the test block:

$$\psi = \frac{\gamma T r_1 r_2}{2L_1(2L_1 + r_1 + r_2)}. \quad (13)$$

(2) *Bond Strength of the Spray Film When Both the Block Weight and Aerodynamic Loads Are Taken into Account.* For rectangular test blocks subject to aerodynamic loads, equation (3) can be converted to

$$P = 14.8 r_1 r_2. \quad (14)$$

The bond stress of the spray film material when both aerodynamic loads and the self-weight of the test block are taken into account can be calculated by combining formula (13) and formula (14):

$$\psi = \frac{r_1 r_2 (\gamma T + 14.8)}{2L_1(2L_1 + r_1 + r_2)}. \quad (15)$$

(3) *Tensile Strength of the Spray Film When Both the Block Weight and Aerodynamic Loads Are Taken into Account.* Assuming that the spray film material at this time is still in the elastic stage and is not damaged by plastic stretching, the spray film area S squeezed out by the test block is as follows:

$$S = 2(r_1 + r_2)l. \quad (16)$$

The tensile stress calculation formula of the spray film material under this condition can be obtained as follows:

$$\xi = \frac{(T\gamma + 14.8)r_1r_2}{2(r_1 + r_2)\sqrt{L_1^2 + h_1^2} \cos \arctan L_1/h_1}. \quad (17)$$

(4) *Tensile Strength of the Spray Film When only the Self-Weight of the Test Block is Considered.* At this point, the aerodynamic load is subtracted in equation (17) to obtain the tensile stress calculation formula for spray film materials that only consider the self-weight of the test block:

$$\xi = \frac{T\gamma r_1 r_2}{2(r_1 + r_2)\sqrt{L_1^2 + h_1^2} \cos \arctan L_1/h_1}. \quad (18)$$

3.4. *The Main Required Mechanical Properties of Spray Film Materials.* The mechanical properties of the spray film material should be calculated according to the most unfavorable circular test block to provide a sufficient safety factor in actual construction. Based on this principle, the calculation results are described below.

3.4.1. Circular Test Block

(1) *When only Self-Weight is Considered.* The calculation results are shown in Table 3.

The results show that the minimum bond strength of the sprayed film material and the lining concrete is positively correlated with the diameter of the falling block. The theoretical analysis suggests that the minimum bond strength requirement is no less than 1.73 MPa and that the minimum tensile strength is no less than 3.45 MPa.

(2) *When Both Self-Weight and Aerodynamic Loads Are Considered.* The calculation results are shown in Table 4. According to the analysis of the calculation results, the single-hole, double-line 100 m² tunnel with a speed of 350 km per hour when trains meet is the most unfavorable working condition. The required minimum bond strength is no less than 3.95 MPa, and the minimum tensile strength is no less than 7.89 MPa.

Considering the aerodynamic effect, the dragging effect of the spray film layer on the falling block, and the use of the spray film layer to ensure that the lining cracks meet the specification limits, it is recommended that the bonding strength of the spray film material and the concrete be no less than 3.95 MPa and that the tensile strength of the spray film material be no less than 7.89 MPa. In addition, if the structure is subjected to a large external force load and needs to meet the crack width limit requirements, the tensile strength of the spray film material still needs to be analyzed according to the specific force situation.

3.4.2. Rectangular Test Block

(1) *When Only Self-Weight is Considered.* The calculation results after the substitution of the parameters are shown in Table 5.

TABLE 3: Mechanical indicators of film spray film materials for circular falling blocks under self-weight.

Nos	Block diameter (m)	Minimum bond strength (MPa)	Minimum tensile strength (MPa)
1	0.5	0.14	0.287
2	1.0	0.29	0.575
3	2.0	0.58	1.150
4	3.0	0.86	1.725
5	4.0	1.15	2.300
6	5.0	1.44	2.875
7	6.0	1.73	3.450

The theoretical analysis suggests that the minimum bond strength requirement is no less than 1.565 MPa and that the minimum tensile strength is no less than 1.69 MPa when only the self-weight of the test block is taken into account.

(2) *When Both the Self-Weight and Aerodynamic Loads Are Considered.* The calculation results are shown in Table 6.

It can be seen that for rectangular lining drop blocks, the bonding strength of the spray film material should not be less than 3.580 MPa and the tensile strength should be no less than 3.865 MPa when considering both the self-weight and aerodynamic load of the test block.

4. Lining Disease Remediation Model Experiment Using Polyurea Spray Film Material

In order to verify the actual strength of the spray film material under the action of the self-weight of the concrete test block and aerodynamic load and whether it can support the tunnel lining block to achieve the purpose of disease remediation, a 1:1 tunnel lining structure model was established at the site to simulate the disease of the tunnel lining block. Through this model experiment, the consistency of the material performance indicators and the theoretical analysis were verified, and the antilining blocking effect of the polyurea spray film material was clarified.

4.1. Model Experiment Scheme

4.1.1. *Purpose of the Experiment.* According to the construction of the tunnel model and the construction process of spray film reinforcement, a total of four working-condition experiments were carried out. The lining thickness was 0.5 m with a rectangular test block of 2 × 3 m in size and a circular test block of $\Phi = 2$ m in diameter. The thickness of the polyurea spray film in each set of test blocks was 5 mm, and the spray film was extended along the edge of the test block for 2 m, as shown in Figure 6. Sandbags were used in the test to simulate aerodynamic loads.

When implemented, the on-site cast-in-place reinforced concrete test model was poured 20 m at a time, and the facility joint was installed every 10 m with a waterstop belt. When the concrete was poured, it was divided by steel plates to form an independent test block, which was suspended

TABLE 4: Spray film bond stress and tensile strength requirements under different circular drop diameters.

No	Block diameter (m)	Minimum bond strength (MPa)	Minimum tensile strength (MPa)
1	0.5	0.33	0.6575
2	1.0	0.66	1.315
3	2.0	1.32	2.630
4	3.0	1.97	3.945
5	4.0	2.63	5.260
6	5.0	3.29	6.575
7	6.0	3.95	7.890

TABLE 5: Mechanical indicators of film spray film materials for rectangular falling blocks under self-weight.

Nos	Block size (m)	Minimum bond strength (MPa)	Minimum tensile strength (MPa)
1	1 × 2	0.381	0.413
2	2 × 3	0.687	0.620
3	3 × 4	0.983	1.062
4	4 × 5	1.275	1.377
5	5 × 6	1.565	1.690

TABLE 6: Spray film bond stress and tensile strength requirements under different rectangular drop sizes.

Nos	Block size (m)	Minimum bond strength (MPa)	Minimum tensile strength (MPa)								
1	1 × 2	0.871	0.945								
2	2 × 3	1.572	1.700								
3	3 × 4	2.248	2.430 </tr <tr> <td>4</td> <td>4 × 5</td> <td>2.916</td> <td>3.149</td> </tr> <tr> <td>5</td> <td>5 × 6</td> <td>3.580</td> <td>3.865</td> </tr>	4	4 × 5	2.916	3.149	5	5 × 6	3.580	3.865
4	4 × 5	2.916	3.149								
5	5 × 6	3.580	3.865								

under the gantry crane after reaching the edge. The polyurea material was sprayed on the inner edge of the arch to simulate the remediation of lining diseases. After the polyurea spray film material reached its strength, the suspension was lifted; thus, the disease of the tunnel lining falling block was simulated. The testing and monitoring was carried out at the same time.

4.1.2. Experimental Conditions. According to the purpose of the model test and the actual service status of the tunnel lining, the shape of the test block was considered according to the most unfavorable consideration. Therefore, the rectangular and circular test blocks were adopted. The experimental conditions are shown in Table 7.

4.2. Model Experimental Structural Design

4.2.1. Model Size. According to the model test scheme, the China Reference Diagram of the Lining Structure of a two-line tunnel at a Speed of 160 km/h was used as the benchmark for the real simulation of the tunnel structure. The inner contour of the tunnel is shown in Figure 7.

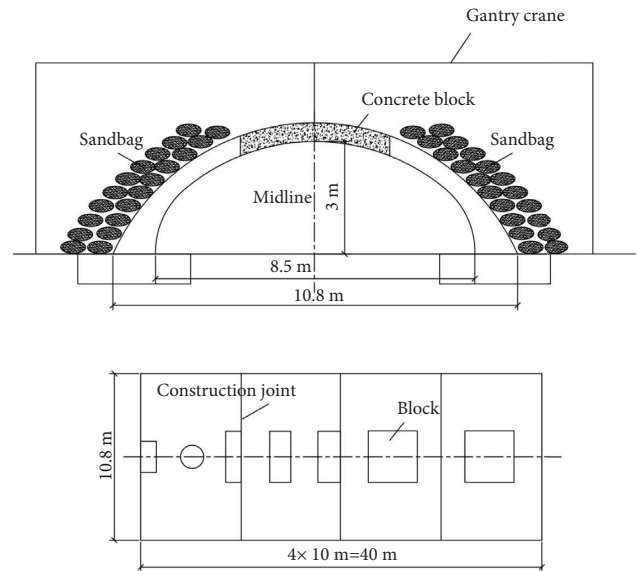


FIGURE 6: Schematic diagram of the model experiment.

We mainly studied the remediation effect of polyurea spray film material on lining block drop disease, focusing on verifying the supporting effect of polyurea spray film material. Due to the certain randomness of the actual tunnel lining block drop disease, the model test considered the most unfavorable working conditions, and the drop block was set with the tunnel vault position. Considering the operating space requirements in the model, the headroom height in the model was set to 3 m, thus determining the model height. Unlike the surrounding rock constraints around the actual tunnel, the bottom of the test model had a large arch foot structure, and a bar foundation and antishear keys were set in the upper part of the arch foot to resist the horizontal thrust of the model arch foot and to ensure safety.

The dimensions of the test model are shown in Figure 8.

4.2.2. Structural Calculation. According to the test scheme, there were two types of loading conditions for the test model: self-weight and self-weight + aerodynamic load. The most unfavorable working conditions were self-weight + aerodynamic load, and the structural calculation was carried out according to this working condition. The additional surface loads formed by personnel and equipment on the surface of the model under the loading conditions were considered at the same time. The structural

TABLE 7: Summary of experimental conditions.

Nos	Block shape	Block size	Spray film thickness (mm)	Epitaxial range (m)	Block weight	Aerodynamic loads	Note
1	Circle	Φ2 m	5	2	√	√	Crack epoxy consolidation + surface epoxy consolidation + the surface is sprayed with polyurea
2	Rectangle	2 × 3 m	5	2	√	√	The surface is sprayed with polyurea
3	Rectangle	2 × 3 m	5	2	√	√	Crack epoxy consolidation, destruction test
4	Circle	Φ2 m	5	2	√	√	Crack epoxy consolidation + surface epoxy consolidation + the surface is sprayed with polyurea, destruction test

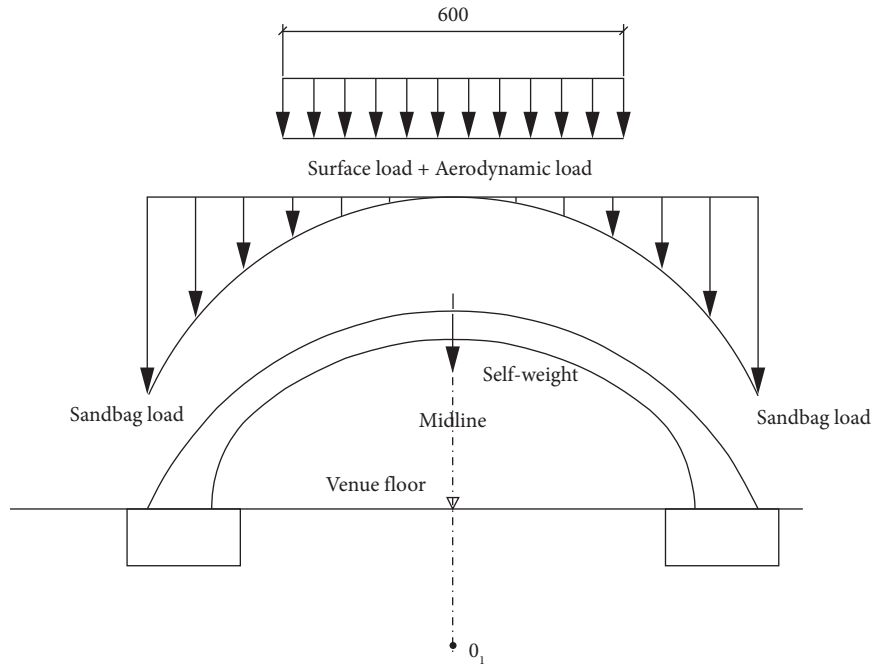


FIGURE 9: The designed model structure load.

TABLE 8: Structural calculation loads.

Model self-weight standard value (kN·m ³)	Aerodynamic loads (kPa)	Additional surface loads for personnel and equipment (kPa)	Sandbag load (kN·m ³)
25	15	10	20

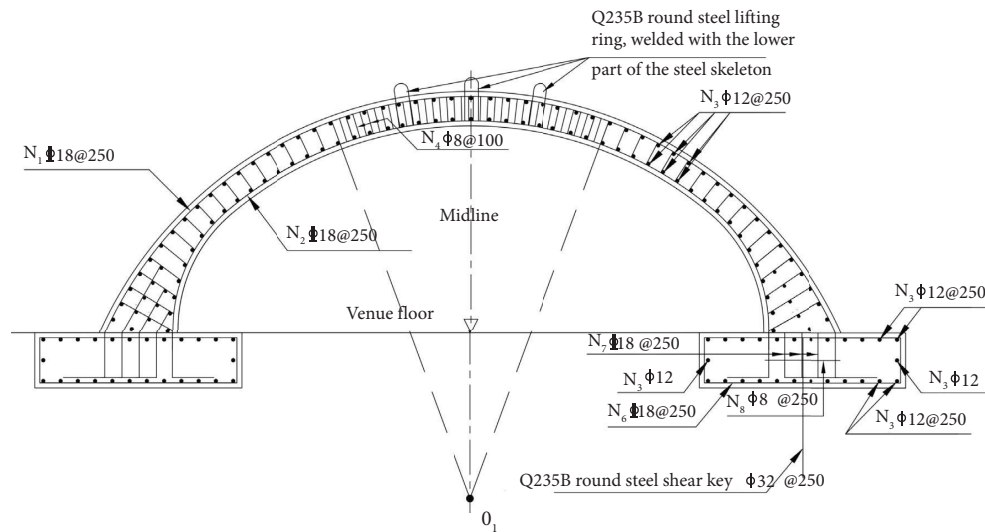


FIGURE 10: Model structure reinforcement diagram.

(2) *Safety Control.* The inside, outside, and test blocks of the tunnel model were fully enclosed and isolated by metal mesh, and safety warning signs were set up to ensure the safety of on-site construction workers and test personnel, as shown in Figure 12.

4.3.2. *Polyurea Material Spraying.* After the base surface treatment of the bottom and edge seam extension of the circular test block, 5 cm of epoxy consolidation material was infused at the edge gap between the test block and the incision. The substrate was sprayed with epoxy

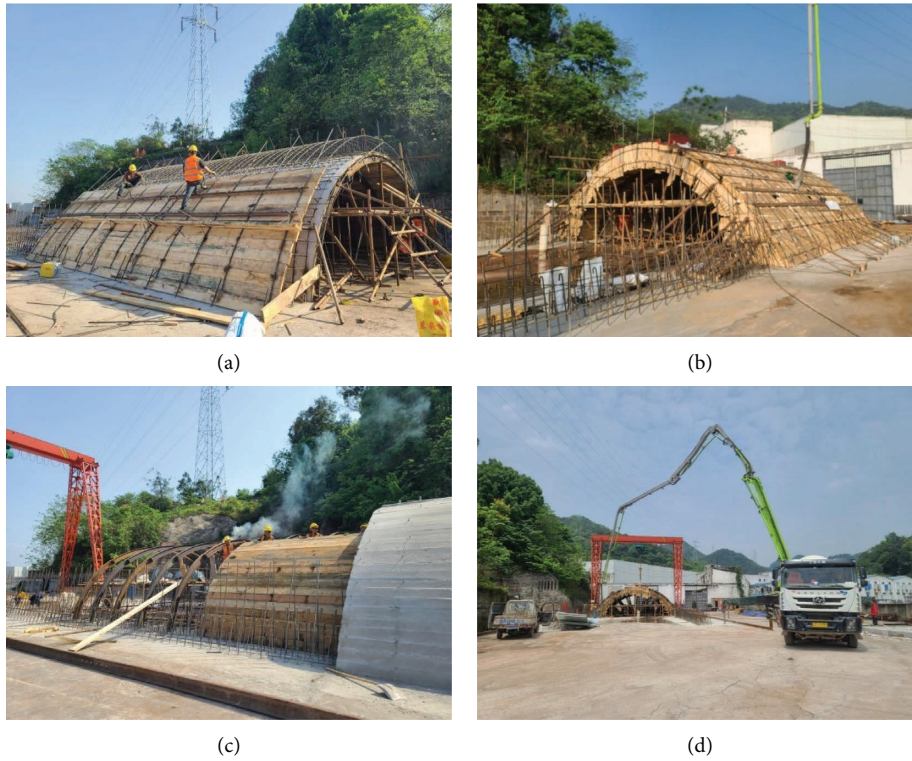


FIGURE 11: Construction of the experiment model. (a) Lining formwork installation of the first plate. (b) Concrete pouring of the first plate. (c) Lining formwork installation of the second plate. (d) Concrete pouring of the second plate.



FIGURE 12: Construction safety control. (a) Tunnel model entrance isolation. (b) Tunnel model internal isolation. (c) The tunnel model was fully enclosed and isolated. (d) Warning signs around the vault test block.

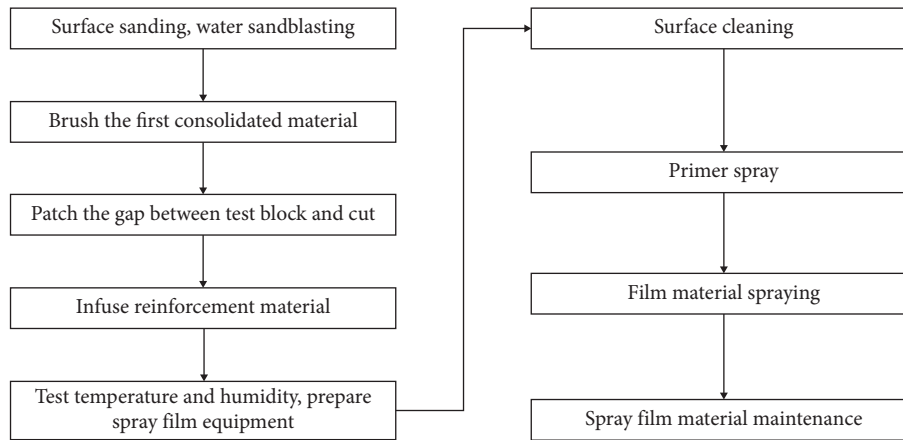


FIGURE 13: Process of polyurea material spraying.

consolidation materials, followed by primers and polyurea spray materials. The specific process is shown in Figures 13–15.

4.4. Simulation Test under Different Working Conditions

4.4.1. Tensile Stress of Polyurea Material Spray Film. The tensile stress of the polyurea spray film material can be analyzed by testing the elastic strain of the spray film material at the measuring point under each loading condition, for which the resistive strain gauges were used to test the elastic strain of the polyurea spray film material under the corresponding loading conditions.

The arrangement of the measuring points for spray film material near the inner surface of the tunnel on the rectangular and circular test blocks and the pasting method of the strain gauges at the measuring points are shown in Figures 16 and 17, respectively.

4.4.2. Block Sinking Measurement. In the model test, the amount of vault sinking and staggering that occurs when the test block of the tunnel arch is supported and reinforced by the spray film material can be tested using a total station and a steel ruler, respectively. The test method for determining the amount of sinking of the test block vault and the amount of misalignment between the test block and the surrounding lining is shown in Figure 18.

The amount of vault sinking h_i can be obtained by measuring the height difference between the tunnel model vault measurement points A , B , and C during the experimental loading process.

4.4.3. Misalignment between the Block and Surrounding Concrete. The misalignment Δh between the test block and the surrounding concrete lining in the tunnel model can be obtained by the displacement amount that occurs before and after the sinking of the test block on measurement points A and B . The specific test method is shown in Figure 19.

5. Experimental Results

5.1. Results of Experimental Condition 1

5.1.1. The Bond Strength between the Polyurea Material and Concrete Surface. According to the test results at different points, the average bond strength of working condition 1 was 3.83 MPa.

5.1.2. Polyurea Material Spray Film Thickness. According to the test results at different points, the average spray film thickness in working condition 1 was 5.7 mm.

5.1.3. Tensile Strain and Stress of Spray Film Material. For the cylindrical test block supported and reinforced by spray film material with a thickness of 5 mm, the largest strain values were at measuring points D and G , as shown in Figure 16(b). The spray film material was in a tensile state along the tunnel ring and in the axis direction. Taking the strain at points D and G as an example, the relationship curve of the longitudinal tensile strain with time at point D is shown in Figure 20, and the relationship curve of the lateral tensile strain with time at point G is shown in Figure 21.

As can be seen from Figures 20 and 21, under the load condition of the test block weight and with an additional load of about 8.6 t, the maximum tensile strain measured at points D and G was $\varepsilon_t = -42.65 \mu\varepsilon$.

According to the field test conditions, the test time under the action of the arch test blocks and sandbags with a self-weight of about 8.6 t lasted for almost 80 min. During this test, the spray film materials were in the linear elastic deformation stage, and no plastic yield or brittle fracturing occurred. The spray film material modulus of tensile elasticity E after curing was about 8 MPa. According to the stress and strain relationship of the spray film material in the elastic stage after curing, the tensile stress σ_t of the central part of the spray film material can be obtained as follows:

$$\sigma_t = E\varepsilon_t, \quad (19)$$

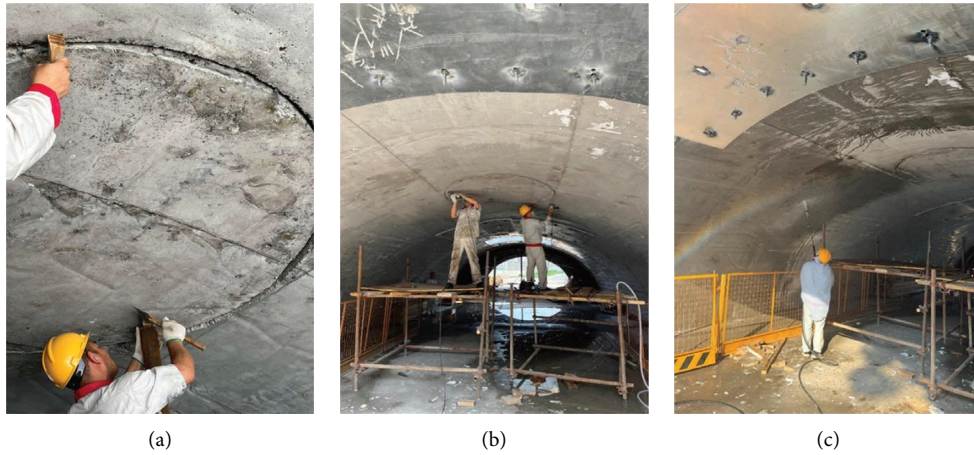


FIGURE 14: Surface treatment. (a) Adjusting the incision. (b) Burnishing. (c) Water sandblasting.

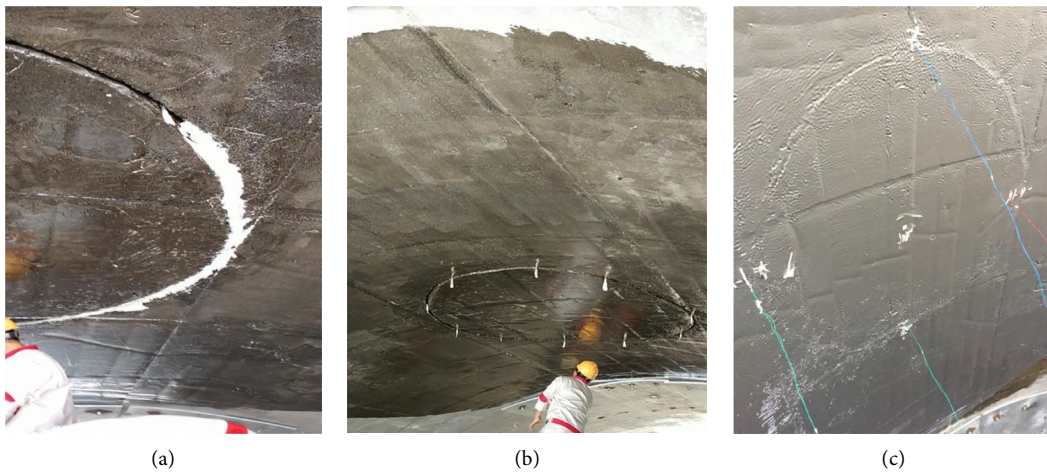


FIGURE 15: Primer spraying. (a) Greasing the side seams. (b) Epitaxial spraying. (c) Final rendering.

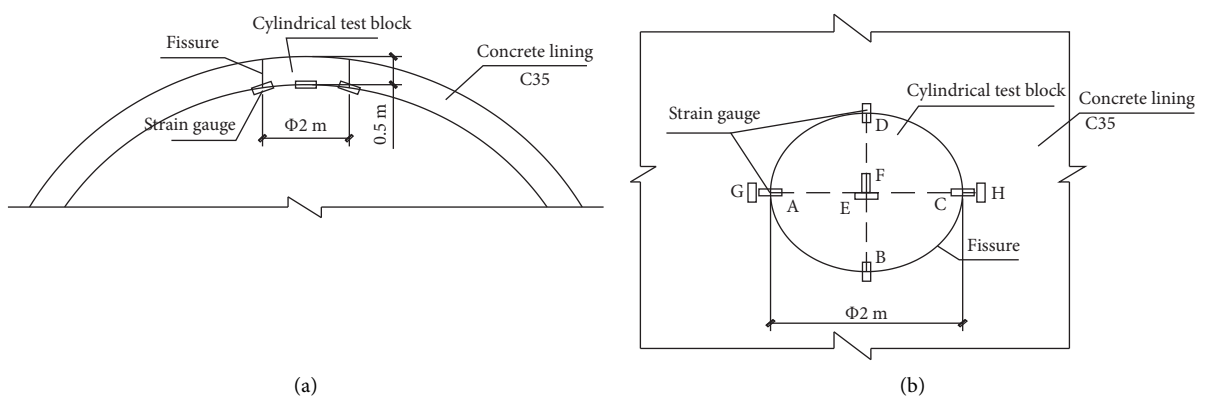


FIGURE 16: Strain measurement points on the spray film material for the circular test block. (a) Front view. (b) Top view.

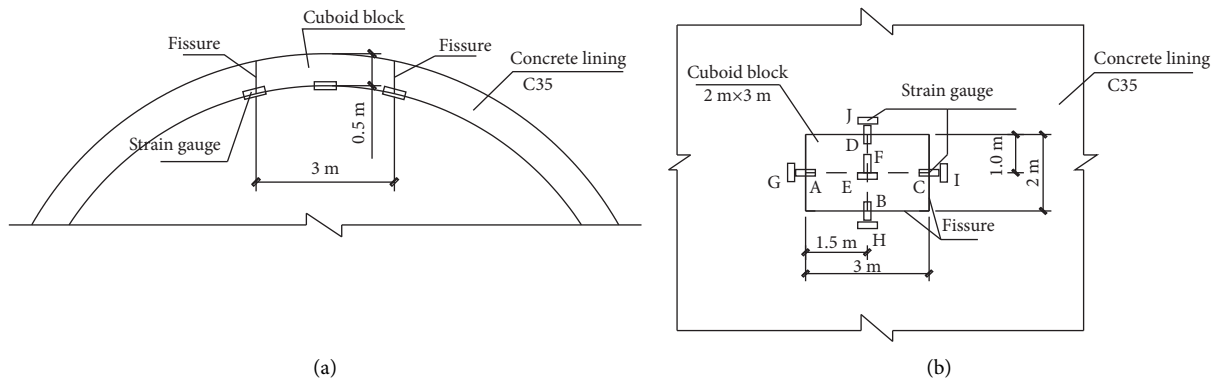


FIGURE 17: Strain measurement points on the spray film material for the rectangular test block. (a) Front view. (b) Top view.

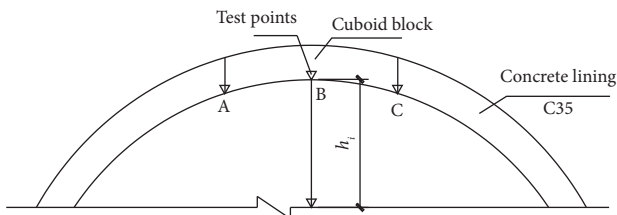


FIGURE 18: Test of lining vault block sinking.

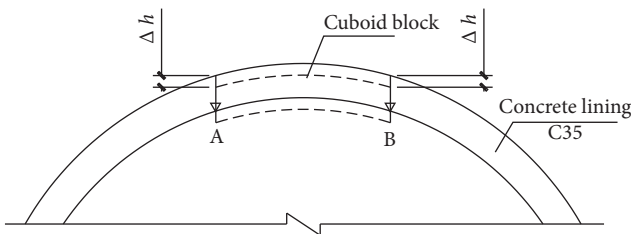


FIGURE 19: Misalignment measurement.

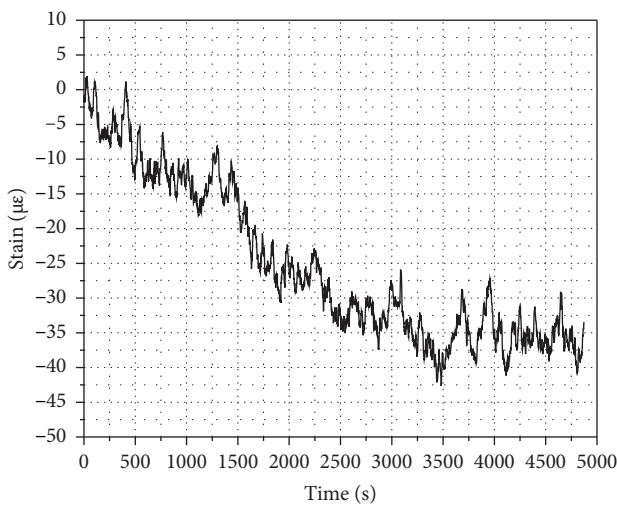


FIGURE 20: Longitudinal tensile strain curve at measurement point D.

where E is the tension elasticity modulus of the spray film material, MPa, and ϵ_t is elastic tensile strain value produced by spray film material, $\mu\epsilon$.

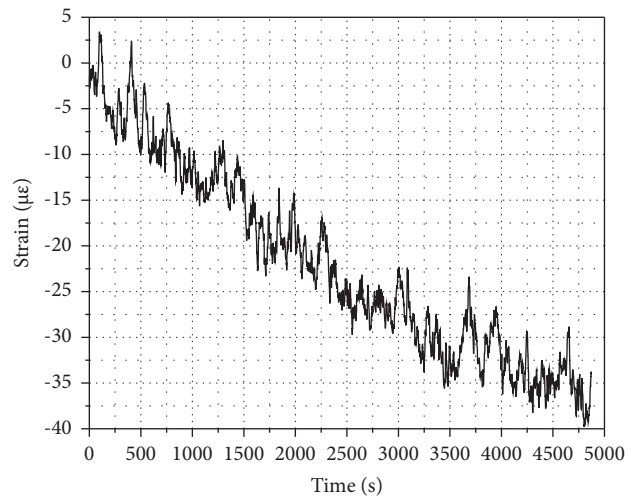


FIGURE 21: Lateral tensile strain curve at measurement point G.

The maximum tensile stress at point D can be calculated by equation (19): $\sigma_t = 0.341$ kPa.

The tensile strength of the spray film material measured in the laboratory was 13 MPa. It can be seen that under the joint action of the $\Phi 2.0$ m cylindrical test block with a sandbag with a weight of about 8.6 t, the maximum tensile stress ($\sigma_t = 0.341$ kPa) of the spray film material with a thickness of 5 mm was much less than the tensile strength.

Due to the infusion of epoxy consolidation materials in the cracks, the adhesion force between the test block and the concrete around it was far greater than the weight of the test block and the load. There were no sinking or misalignment phenomena in the test block after the sling was detached. Therefore, the role of the spray polyurea in lifting the test block and the total weight of the load was not played out at all.

It was found that the 5 mm thick spray film material in the test could withstand a cylindrical test block of $\Phi 2 \times 0.5$ m and an aerodynamic load of 8.6 t. The tensile stress was much smaller than the tensile strength, and no tensile yield or brittleness failure occurred in the spray film material during the test.

The stress analysis of the spray film material tested in working condition 1 showed that the spray film material with a thickness of 5 mm was pulled along the tunnel loop

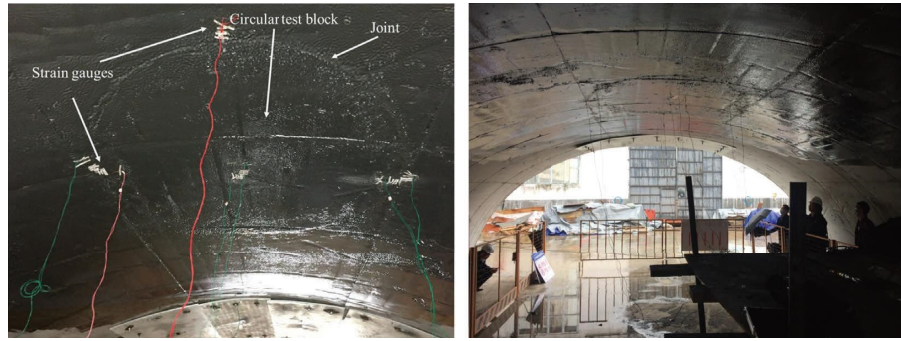


FIGURE 22: The state of the spray film material in the inner wall of the tunnel after loading.

and the tunnel axis under the combined effect of the test block gravity and the aerodynamic effect of the high-speed railway tunnel. The spray film material was in a tensile state, and the maximum tensile stress at the measuring point was less than the tensile strength of the spray film material.

5.1.4. Misalignment between the Block and Lining. Because the test block did not sink during loading condition 1, its sinking amount was zero, and the amount of misalignment was also zero. The condition of the spray film surface during loading is shown in Figure 22.

Based on the model test of the tunnel lining reinforced with a spray film material with a thickness of 5 mm, combined with the analysis of the strain and stress test, the following conclusions were reached. The tensile stress was between 0.264 and 0.341 kPa under the action of the lining arch drop and the aerodynamic effect of the high-speed railway tunnel with a load of 8.6 t on the spray film material with a thickness of 5 mm. The spray film material was in a pulled state along the tunnel ring and the tunnel axis. The tensile stress of the 5 mm spray film material in the model test condition was less than its tensile strength of 13 MPa. This shows that the spray film material with a thickness of 5 mm was able to bear the combined effect of the tunnel arch lining block and aerodynamic effect without shear or tensile failure in test condition 1.

5.2. Results of Experimental Condition 2

5.2.1. Bond Strength. According to the test results at different points, the average bonding strength of working condition 2 was 4.5 MPa.

5.2.2. Polyurea Material Spray Film Thickness. According to the test results at different points, the average polyurea spray film thickness in condition 2 was 5.6 mm.

5.2.3. Tensile Strain and Stress of Spray Film Material. The dimensions of the rectangular test block used to simulate the lining of the tunnel arch in condition 2 were $2.0 \times 3.0 \times 0.5$ m. In the test of the spray film material it strained under the combined action of the block self-weight and the aerodynamic effect. The 5 mm thick spray film

material was affected by internal tension stress during loading. At the beginning of the loading, the internal tensile strain and compressive strain were small. The tensile and compressive strain values of each measurement point changed greatly with the increase in the applied loads, and the compressive stress changed from compressive stress to tensile stress. The maximum tensile strain in the spray film material occurred at the moment when the test block was close to sinking. According to the analysis of the spray film material strain value at each measurement point, shown in Figure 17, the strain values at the three points of measurement points *A*, *H*, and *J* were the largest. In the process of loading the spray film material until it sank, the spray film materials at measuring points *A*, *H*, and *J* were in a state of tensile stress. The tensile strain curves for measuring points *A*, *H*, and *J* are shown in Figures 23(a)–23(c), respectively.

As can be seen from Figure 23, under the loading condition of being subjected to the block's own weight and the weight of 14 t sandbags, the maximum tensile strain of the polyurea spray film material measured was $63334.11 \mu\epsilon$.

According to working condition 2 of the field test, the test time under the weight of the arch test block and the sandbag with a load of about 14 t lasted for nearly 50 min. The spray film material was in the linear elastic deformation stage during the sinking process of the test block, and no brittle fracturing occurred. The tensile elastic modulus was $E = 8$ MPa after the spray film material was cured, thus obtaining the maximum tensile stress of $\sigma_t = 506.7$ kPa.

The tensile strength of the sprayed film material was 13 MPa. It can be seen that under the combined action of a test block of $2.0 \times 3.0 \times 0.5$ m and a sandbag with a weight of about 14 t, the maximum tensile stress of the spray film material with a thickness of 5 mm during the sinking process of the test block was 506.7 kPa. This is still less than the tensile strength of the spray film material of 13 MPa.

In case 2, the test block sank during loading and peeled off the spray film material within a certain range around the test block. This phenomenon indicates that the bond strength between the spray film polyurea material and the tunnel lining concrete surface reduced gradually, which, in turn, caused the spray film polyurea material to be stripped from the surface of the concrete by the sinking test block.

For the spray film material with a thickness of 5 mm in case 2, it was subjected to pressure and tensile stress before

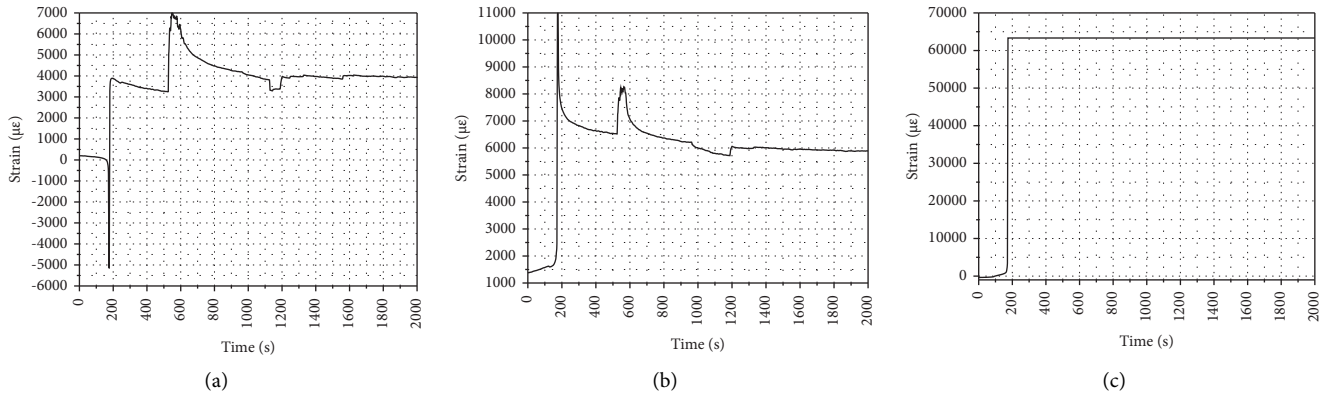


FIGURE 23: The relationship between strain and time of spray film material. (a) Measurement point A. (b) Measurement point H. (c) Measurement point J.

the test block sank under the combined action of the self-weight of the rectangular test block and the simulated aerodynamic effect of the high-speed railway tunnel with a load of about 14 t. When the test block sank, the spray film material was all in a state of tensile stress, but the maximum tensile stress obtained by the test was still less than the tensile strength of the spray film material.

The thickness of the spray film material in this loading test was 5 mm. Although there was a sinking phenomenon for the test block in condition 2 during loading, the tensile stress in the spray film material did not exceed its tensile strength during the sinking period. The failure phenomenon of tension cracking and tearing did not occur on the spray film material, which showed that the spray film material with a thickness of 5 mm in condition 2 could withstand and drag the sinking test block to prevent it from falling to the floor completely. The main reason for the sinking of the test block during loading may be due to the decrease in bond strength between the spray film material and the concrete wall, and the bonding tension caused by the increased weight of the test block could not be resisted. Therefore, in order to prevent the tunnel lining arch test block from falling, measures such as increasing the bond strength between the spray film material and the concrete or increasing the thickness of the spray film material can be taken.

5.2.4. Test Block Misalignment and Spray Film Material Peeling Area. During the model test, the arch cube test block sank under the combined action of its self-weight and the simulated aerodynamic effect loads, but it did not fall to the ground completely. Between the test block and the tunnel lining, there was a misalignment. The maximum settlement of the concrete block tested on-site was 29 cm, and the maximum amount of misalignment between the test block and the surrounding concrete lining was 28 cm. Due to the sinking of the test block during loading, the spray film material around the test block was stripped from the tunnel concrete lining, as shown in Figures 24–26.

The sinking amount and misalignment of the test block in condition 2 is shown in Figure 27. The maximum



FIGURE 24: The condition of the cuboid test block after sinking.

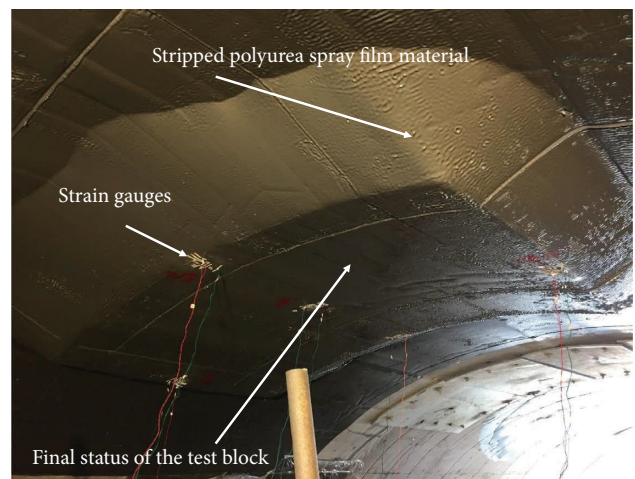


FIGURE 25: The tensile status of the spray film material after the test block sank.

settlement of the test block was 29 cm, and the misalignment between the test block and the surrounding concrete lining reached 28 cm.

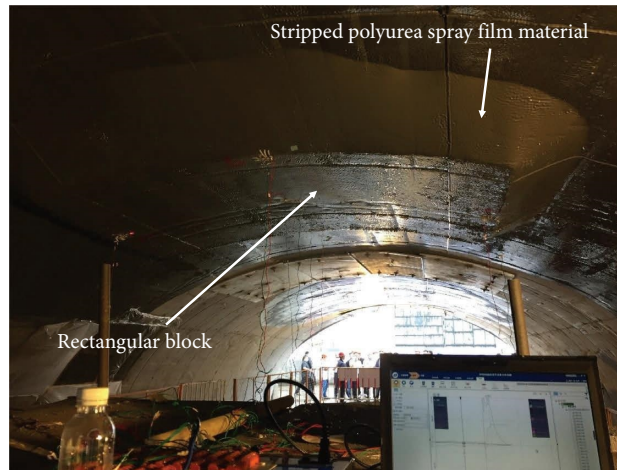


FIGURE 26: The final status of the sunken test block and the stripped spray film material.

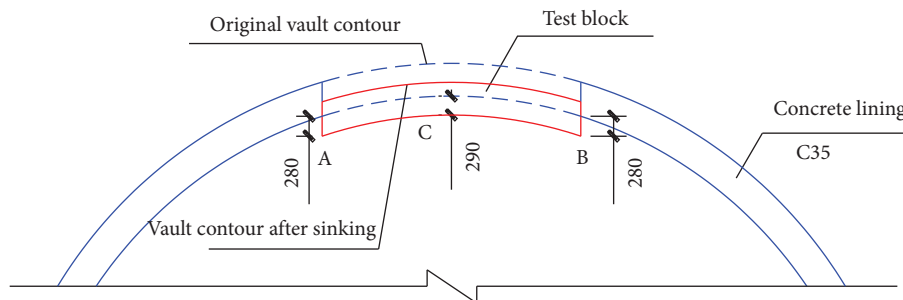


FIGURE 27: Misalignment between the block and surrounding lining (mm).

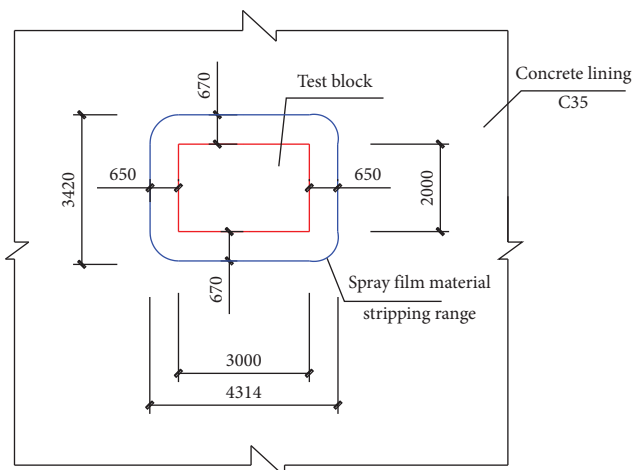


FIGURE 28: Floor plan of the peeling range of the spray film material around the rectangular test block (mm).

According to the field test, the floor plan of the stripped spray film material area around the $3 \times 2 \times 0.5$ m rectangular test block is shown in Figure 28.

It can be seen from Figure 28 that the length of the slope of the spray film material that peeled off along the sinking of the test block was about 0.65 to 0.67 m on the horizontal plane. The projection of the spray film material sinking with

the test block on the horizontal plane was a rectangle of 3.42×4.31 m. From this, it can be calculated that the area of the spray film material stripped from the concrete lining was about 8.6 m^2 .

The cross-section of the spray film material around the test block peeled off from the lining due to the weight of the test block and sandbag load is shown as Figure 29.

From Figure 29, it can be concluded that the peeling spray film material around the test block in condition 2 was within 1.0 m.

According to the model test of the spray film material with a thickness of 5 mm used to prevent the tunnel lining falling block disease under working condition 2, the following conclusions can be made:

- (1) For the test block in working condition 2, when the 5 mm thick spray film material's extension range was 2 m, the tensile stress caused by the block drop was 506 kPa under the action of the block's self-weight and the aerodynamic effect of the high-speed railway tunnel of about 14 t. The spray film material was in a tensile and compressive state along the tunnel ring and the tunnel axis during the loading test, and the tensile stress was greater than the compressive stress. The whole spray film material was in a tensile stress state after the test block sank. The maximum tensile stress of the spray film material in model test case 2

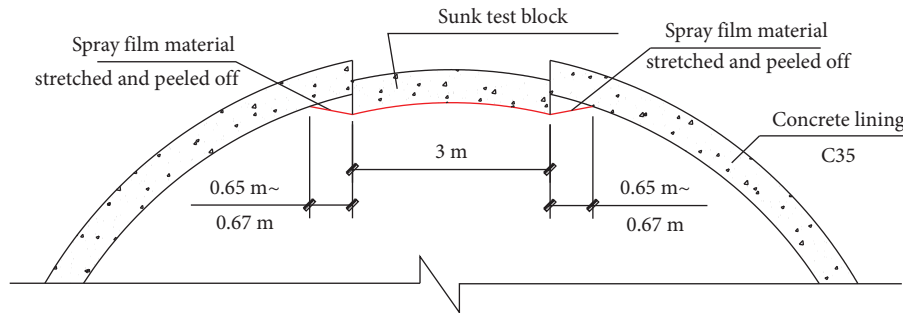


FIGURE 29: The spray film material that was peeled off around the periphery of the sunken cuboid test block.

was less than its tensile strength (13 MPa). This indicates that the spray film material with a thickness of 5 mm can bear the combined effect of the tunnel arch lining block drop and the aerodynamic effect without shear or tensile failure.

- (2) The use of 5 mm thick spray film material failed to prevent the concrete test block from sinking in model test condition 2, but the test block did not fall to the floor of the tunnel completely and was dragged and supported by the stripped spray film material. After the test block sank, the misalignment between the test block and the surrounding concrete lining reached 28 cm, and the area of the spray film material on the inner wall surface of the model tunnel concrete lining was about 8.6 m² due to the sinking and pulling of the test block.
- (3) It can be concluded that the reason for the block sinking was related to the decrease in the bond strength between the spray film material around the test block and the concrete. The range of the stripped film material around the test block was less than 1.0 m. Therefore, it is recommended that the bond strength between the spray film material and the concrete within 1.0 m of the spraying range around the test block should be appropriately increased. In addition, in order to reduce the tensile stress concentration caused by the uneven thickness of the spray film material due to the spraying construction process, it is recommended that the thickness of the spray film material should be appropriately increased.

5.3. Results of Experimental Condition 3. The test block in condition 3 was a cuboid block of 2 × 3 × 0.5 m. In this condition, the cracks between the test block and the surrounding concrete were treated with perfusion epoxy and were not reinforced with spray film material. Therefore, only destructive loading tests were performed on the shear-to-vandal resistance of the perfused epoxy material. However, the test block did not sink or fall under the action of its own weight or under the weight of the upper sandbag with a total load of 11.5 t during the loading period. Under the action of the 11.5 t load, the perfusion of the epoxy material was free of destruction. The test block in condition 3 did not sink or misalign, and its test value was zero.

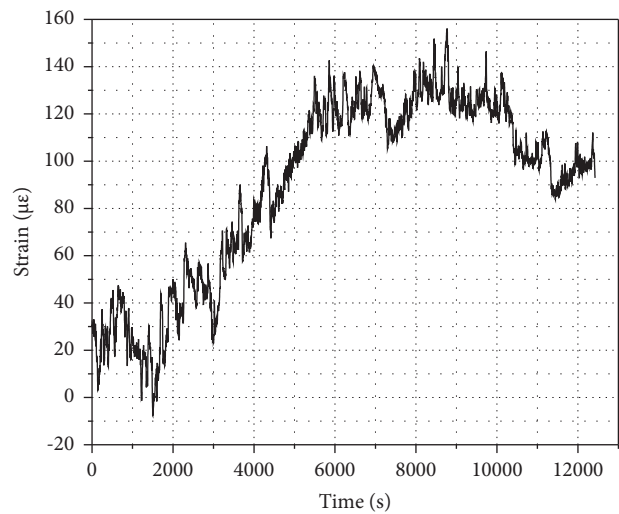


FIGURE 30: Strain curve at point B.

5.4. Results of Experimental Condition 4

5.4.1. Tensile Strain and Stress of Spray Film Material. The loading test for working condition 4 consisted of spraying 5 mm thick polyurea material in the arch of the tunnel model and repairing the cracks between the test block and the concrete lining with infused epoxy material. The test block was a circular block of $\Phi 2 \times 0.5$ m. The loads on the cylindrical test block included its own weight and the additional loads applied by the sandbag on its upper part, and then the load carrying capacity of the spray film material under the two loads was analyzed.

The strain values at measurement points B and C were the largest for the cylinder test block of $\Phi 2 \times 0.5$ m, shown in Figure 16. The spray film material was in a tensile state along the tunnel ring and axis direction. The relationship curve of the longitudinal tensile strain at point B is shown in Figure 30.

As can be seen from Figure 30, the maximum tensile strain measured by the spray film material with a thickness of 5 mm at point B and point C under a sandbag load of about 9.5 t was $\epsilon_t = 156.03 \mu\epsilon$.

According to the conditions of the field test, the test lasted for nearly 250 min under the combined action of the arch test block weight and a sandbag load of about 9.5 t. The spray film material was in the linear elastic deformation



FIGURE 31: The appearance of the spray film material of the tunnel arch cylinder test block. (a) Before loading. (b) After loading.

stage during the test, and no plastic yield or brittle fracturing occurred, nor did any significant sinking or falling appear.

The tensile elastic modulus was $E = 8$ MPa after the spray film material was cured. According to the stress and strain relationship of the spray film material in the elastic stage after curing, it was calculated from equation (19) that the maximum tensile strain was $\varepsilon_t = 156.03 \mu\varepsilon$. At the peripheral measuring point B , the tensile stress was $\sigma_t = 1.25$ kPa. The tensile strength of the sprayed film material was 13 MPa. It can be seen that under the combined action of the $\Phi 2.0$ m cylindrical test block weight and a total sandbag weight of about 9.5 t, the maximum tensile stress ($\sigma_t = 1.25$ kPa) borne by the spray film material with a thickness of 5 mm was much less than the tensile strength of the spray film material.

It was found that the spray film material with a thickness of 5 mm in working condition 4 of the loading test was able to support the joint action of the cylindrical test block of $\Phi 2 \times 0.5$ m and an additional load of about 9.5 t. The tensile stress of the spray film material was much less than its tensile strength, and the spray film material did not undergo tensile yield or brittle damage during the test, nor was there any significant sinking or falling.

5.4.2. Misalignment between the Block and Surrounding Concrete. After the misalignment test on the lower arch test block supported and reinforced by a 5 mm thick spray film material, the arch test block in model test condition 4 did not sink or fall during loading. The sinking amount was zero, and the amount of misalignment was also zero. The spray film material was not peeled off from the inner wall of the concrete. The condition of the spray film surface during loading is shown in Figure 31.

From the test in experimental condition 4, the following conclusions can be addressed: In the destructive test simulating the action of the railway tunnel lining arch block falling under an additional aerodynamic load of about 9.5 t, the tensile stress test value inside the spray film material was between 0.76 and 1.25 kPa. The spray film material was under tensile stress along both the tunnel ring and the tunnel axis. The tensile stress of the spray film material in the test

was less than its tensile strength of 13 MPa, indicating that the spray film material with a thickness of 5 mm in this destructive test was still able to bear the joint effect of the block weight and tunnel aerodynamic effect in the model tunnel. The spray film material did not have tensile or shear damage, and the cylindrical test block did not sink or fall.

6. Discussion

For all of the four model tests, only the spray film under working condition 2 fell off. Therefore, the mechanical properties of the spray film material under working condition 2 need to be verified.

6.1. Validation of the Assumptions in the Calculation of the Spray Film Material Bond Strength. The length and width of the rectangular test block were as follows: $r_1 = 3$ m, $r_2 = 2$ m; the thickness of the block: $T = 0.5$ m; the bulk weight of the block: $\gamma = 23$ kN/m³; the simulated aerodynamic load: $P = mg = 14 \times 9.8 = 137.2$ kN; and the average width of the spray film material bevel that peeled off as the test block sank projecting on the horizontal plane: $L_1 = 0.66$ m. According to the measured data, the actual bond strength of the spray film material can be calculated by equation (15).

$$\psi = \frac{2 \times 3 \times 23 \times 0.5 + 137.2}{2 \times 0.66 \times (2 \times 0.66 + 2 + 3)} = 24.72 \text{ kPa.} \quad (20)$$

From Table 6, for rectangular concrete test blocks with a length \times width = 3 \times 2 m, the theoretical bond strength of the polyurea spray film material was 1.572 MPa. The measured value is only 1.57% of the theoretical value. The calculations show that the supporting effect provided by the material after actual construction was much smaller than the theoretical analysis value. On the other hand, the average bond strength of the spray film material under the measured working conditions was 4.5 MPa. The test results had values much greater than the calculated values, but the polyurea spray film material failed in experimental condition 2. In view of the above situation, the reasons for this are analyzed as follows:

6.1.1. Differences between the Measured Bond Strength Calculation and the Theoretical Bond Strength Calculation

- ① Reasonableness of the assumptions regarding the stressed region of the spray film material:

In the theoretical analysis of Section 3.3.1, the force area of the spray film material's bond strength was assumed to be 0.01 m outside the boundary of the falling block. The actual measured spray film peeling width was 0.66 m, which is 66 times the hypothesized value. Therefore, the hypothesized value is conservative.

- ② Reasonableness of the aerodynamic load assumptions:

In the theoretical analysis, the aerodynamic load of 88.8 kN for double trains meeting at a speed of 350 km/h was given to calculate the bond strength between the spray film material and the lining concrete surface. In the model test, the aerodynamic load was simulated by accumulating 14 t sandbags, with a load of 137.2 kN. The dynamic load of the model test was 1.55 times that of the theoretical assumption, so the assumed load is small.

- ③ Reasonableness of the elasticity hypothesis:

The theoretical calculations assumed that the polyurea spray film material was still in the elastic deformation stage when peeling. However, plastic damage may occur in the spray film material during actual engineering. The elasticity assumption may therefore not be satisfied. In addition, the theoretical calculation assumed that the supporting area of the entire spray film material was evenly stressed. However, the spray film was the most stressed at the edge of the contact between the test block and the lining. There was a decreasing trend along the edge of the spray film material.

6.1.2. Differences between the Measured Bond Strength and the Calculated Bond Strength

- ① Test position. The actual bond strength failure occurred in the side seam position. However, in order to conduct bond strength tests, a small part of the membrane material is destroyed. To avoid this, the test position was far from the side seam. Therefore, the bond strength of the seam position in condition 2 was not detected. Affected by the test method, the bond strength of the spray film material was not measured at the edge of the test block, that is, at the most dangerous A and A' points in Figure 1. Therefore, the measured values were much larger than the theoretically calculated values.
- ② Side seam treatment process. The width of the side seam was about 1.5 cm in working condition 2. The surface of the side seam was irregular, and more special putty was used for screeding. The strength of the putty selected for the test was low, and the adhesion strengths of the primer and the film material

did not match. This resulted in the special putty being peeled off from the concrete surface first, then causing the local peeling of the membrane material. The low strength of the special putty is one of the main reasons for the failure of the local bonding strength.

- ③ Surface sanding process. The particle size and strength of the quartz sand used in condition 2 were small. Additionally, the grinding time was short. Therefore, the surface grinding process was one of the main reasons for the failure of local bond strength in condition 2.

6.2. Validation of the Assumptions in the Calculations of the Spray Film Material Tensile Strength. The amount of rectangular test block misalignment was $h_1 = 0.28$ m. As can be seen from equation (16), the theoretical calculation of the tensile stress ξ of the spray film material at this time is as follows:

$$\xi = \frac{2 \times 3 \times 23 \times 0.5 + 137.2}{2 \times (2 + 3) \times \sqrt{0.66^2 + 0.28^2} \times \cos \arctan L_1/h_1} \quad (21)$$

$$= 103.1 \text{ kPa.}$$

The maximum tensile stress of the spray film material measured in Section 5.2 was 506.67 kPa, which shows that the tensile stress of the spray film material measured in the model test was 4.9 times that of the theoretical calculation result. The actual tensile stress was much greater than the tensile strength of the spray film material, so the spray film material was destroyed.

7. Conclusions

In this study, a model test of the polyurea spray film material used to prevent lining block from falling was carried out. Four different working conditions were set up, and the bond strength and tensile strength of the spray film material under each working condition were measured. According to the actual measurement results, the proposed theoretical calculation model was verified. According to the results of this study, the following main conclusions can be made:

- (1) After crack epoxy consolidation + surface epoxy consolidation + surface spray polyurea treatment, the average bonding strength measured was 3.83 MPa and the maximum tensile stress was 0.341 kPa. This bonding strength could bear the joint action of tunnel arch lining block drop and the aerodynamic effect without shear or tensile damage. The test block did not fall, and the spray film material was not peeled off.
- (2) After the surface spray polyurea treatment, the average bonding strength measured was 4.5 MPa, and the maximum tensile stress was 506.7 kPa. Under the combined action of the test block's self-weight and an aerodynamic effect of about 14 t load, the tensile stress was less than the tensile strength, and no

tensile fracture occurred in the spray film material during the test.

- (3) The test block sank during the loading process, and the spray film material within a certain range around the test block was peeled off, indicating that the bond strength within the peeling range between the spray film polyurea material and the tunnel lining concrete surface was gradually reduced. In order to prevent the tunnel lining arch test block from falling, measures such as increasing the bond strength between the spray film material and the concrete or increasing the thickness of the spray film material are recommended to be taken.
- (4) The theoretical supporting force of the polyurea spray film material is 1.572 MPa, but the measured value is only 1.57% of the theoretical value. The calculation shows that the supporting effect provided by the material in the actual construction was much smaller than the theoretical analysis value. The maximum tensile stress of the spray film material was 506.67 kPa, and the tensile stress of the spray film material measured in the model test was 4.9 times that of the theoretical calculation result.
- (5) After the crack epoxy consolidation treatment, the test block was able to withstand its own weight and the weight of the upper sandbag for a total load of 11.5 t without sinking or falling.
- (6) After crack epoxy consolidation + surface epoxy consolidation + surface spray polyurea treatment, the maximum tensile stress measured was 1.25 kPa, which was much less than the tensile strength of the spray film material.

Data Availability

The data used to support the findings of this study are included within the article.

Conflicts of Interest

The authors declare that they have no conflicts of interest.

Acknowledgments

The National Natural Science Foundation of China: 51274145.

References

- [1] H. S. Cheng, W. Ang, and H. S. Xiao, "Research on the movement law and traffic safety zoning of spalled blocks in the linings of high-speed railway tunnels," *Tunnelling and Underground Space Technology*, vol. 128, Article ID 104614, 2022.
- [2] L. Li, M. G. Duan, and Z. Cao, "Rehabilitation of highway procedures," *Proceedings of ATTES-ITA 2001 world tunnel Tunnels-Techniques and congress*, pp. 45–50, 2005.
- [3] X. S. Li, Q. H. Li, Y. J. Hu et al., "Study on three-dimensional dynamic stability of open-pit high slope under blasting vibration," *Lithosphere*, vol. 2021, Article ID 6426550, 2022.
- [4] D. Ren, X. Wang, Z. Kou et al., "Feasibility evaluation of CO₂ EOR and storage in tight oil reservoirs: a demonstration project in the Ordos Basin," *Fuel*, vol. 331, Article ID 125652, 2023.
- [5] M. C. He, Q. R. Sui, M. N. Li, Z. J. Wang, and Z. G. Tao, "Compensation excavation method control for large deformation disaster of mountain soft rock tunnel," *International Journal of Mining Science and Technology*, vol. 32, no. 5, pp. 951–963, 2022.
- [6] C. Zhu, X. Xu, and X. T. Wang, "Experimental investigation on nonlinear flow anisotropy behavior in fracture media," *Geofluids*, vol. 2019, Article ID 5874849, 9 pages, 2019.
- [7] Q. Wang, B. Jiang, S. Xu et al., "Roof-cutting and energy-absorbing method for dynamic disaster control in deep coal mine," *International Journal of Rock Mechanics and Mining Sciences*, vol. 158, Article ID 105186, 2022.
- [8] Q. Wang, S. Xu, Z. Xin, M. He, H. Wei, and B. Jiang, "Mechanical properties and field application of constant resistance energy-absorbing anchor cable," *Tunnelling and Underground Space Technology*, vol. 125, Article ID 104526, 2022.
- [9] Q. Yin, J. Wu, Z. Jiang et al., "Investigating the effect of water quenching cycles on mechanical behaviors for granites after conventional triaxial compression," *Geomechanics and Geophysics for Geo-Energy and Geo-Resources*, vol. 8, no. 2, 2022.
- [10] G. Feng, X. Wang, Y. Kang, and Z. Zhang, "Effect of thermal cycling-dependent cracks on physical and mechanical properties of granite for enhanced geothermal system," *International Journal of Rock Mechanics and Mining Sciences*, vol. 134, Article ID 104476, 2020.
- [11] T. Meng, X. Yongbing, J. Ma et al., "Evolution of permeability and microscopic pore structure of sandstone and its weakening mechanism under coupled thermo-hydro-mechanical environment subjected to real-time high temperature," *Engineering Geology*, vol. 280, Article ID 105955, 2021.
- [12] G. Feng, X. Wang, M. Wang, and Y. Kang, "Experimental investigation of thermal cycling effect on fracture characteristics of granite in a geothermal-energy reservoir," *Engineering Fracture Mechanics*, vol. 235, Article ID 107180, 2020.
- [13] P. Jin, Y. Hu, J. Shao, Z. Liu, G. Feng, and S. Song, "Influence of temperature on the structure of pore-fracture of sandstone," *Rock Mechanics and Rock Engineering*, vol. 53, no. 1, pp. 1–12, 2020.
- [14] B. Chiaia, A. P. Fantilli, and P. Vallini, "Combining fiber-reinforced concrete with traditional reinforcement in tunnel linings," *Engineering Structures*, vol. 31, no. 7, pp. 1600–1606, 2009.
- [15] G. Feng, Y. Kang, F. Chen, Y. Liu, and X. Wang, "The influence of temperatures on mixed-mode (I + II) and mode-II fracture toughness of sandstone," *Engineering Fracture Mechanics*, vol. 189, pp. 51–63, 2018.
- [16] E. S. Bernard, "Influence of geometric factors on the punching load resistance of early-age fibre reinforced shotcrete linings," *Tunnelling and Underground Space Technology*, vol. 26, no. 4, pp. 541–547, 2011.
- [17] Y. C. Chiu, C. H. Lee, and T. T. Wang, "Lining crack evolution of an operational tunnel influenced by slope instability," *Tunnelling and Underground Space Technology*, vol. 65, pp. 167–178, 2017.
- [18] H. M. Kroetz, N. A. Do, D. Dias, and A. T. Beck, "Reliability of tunnel lining design using the Hyperstatic Reaction Method," *Tunnelling and Underground Space Technology*, vol. 77, pp. 59–67, 2018.

- [19] K. Tsuno and K. Kishida, "Evaluation of spalling of concrete pieces from tunnel lining employing joint shear model," *Tunnelling and Underground Space Technology*, vol. 103, Article ID 103456, 2020.
- [20] J. Du, Q. Fang, G. Wang, D. Zhang, and T. Chen, "Fatigue damage and residual life of secondary lining of high-speed railway tunnel under aerodynamic pressure wave," *Tunnelling and Underground Space Technology*, vol. 111, no. 5, Article ID 103851, 2021.
- [21] D. Feng, X. Wang, and B. Zhang, "Improving reconstruction of tunnel lining defects from ground-penetrating radar profiles by multi-scale inversion and bi-parametric full-waveform inversion," *Advanced Engineering Informatics*, vol. 41, Article ID 100931, 2019.
- [22] K. Lee, D. Kim, S. H. Chang, S. W. Choi, B. Park, and C. Lee, "Numerical approach to assessing the contact characteristics of a polymer-based waterproof membrane," *Tunnelling and Underground Space Technology*, vol. 79, pp. 242–249, 2018.
- [23] K. Kovari, "History of the sprayed concrete lining method—part II: milestones up to the 1960 s," *Tunnelling and Underground Space Technology*, vol. 18, no. 1, pp. 71–83, 2003.
- [24] J. Kwasny and T. A. Aiken, "Sulfate and acid resistance of lithomarge-based geopolymer mortars," *Construction & Building Materials*, vol. 166, 2018.
- [25] S. Heidari, F. Esmailzadeh, D. Mowla, and S. Ghasemi, "Synthesis of an efficient copolymer of acrylamide and acrylic acid and determination of its swelling behavior," *Journal of Petroleum Exploration and Production Technology*, vol. 8, no. 4, pp. 1331–1340, 2018.
- [26] R. P. Johnson, F. E. Swallow, and S. Psomas, "Structural properties and durability of a sprayed waterproofing membrane for tunnels," *Tunnelling and Underground Space Technology*, vol. 60, pp. 41–48, 2016.
- [27] C. Angeloff, E. P. Squiller, and K. E. Best, "Two-component aliphatic polyurea coatings for high productivity applications," *Journal of Protective Coatings and Linings*, vol. 19, no. 8, pp. 42–47, 2002.
- [28] Z. Bo, *Study on the Corrosion Resistance of Anti-corrosion Coatings in Different Corrosive Environments*, Qingdao Technological University, Shandong, China, 2013.
- [29] P. Lü, G. Chen, and W. Huang, "Study on accelerated aging behavior of polyurea coatings of polyaspartate," *Journal of Sichuan University (Medical Science Edition): Engineering Science Edition*, vol. 39, no. 2, p. 6, 2007.
- [30] Y. Liu, *Research on the Properties and Test Methods of concrete Protective Coatings*, China Academy of Building Materials Science, Beijing, China, 2004.
- [31] H. Yang, *Effect of Sprayed Polyurea Elastomer on concrete Durability*, Qingdao Institute of Civil Engineering and Architecture, Shandong, China, 2004.
- [32] Z. Li, J. Zhang, and W. Huang, "Application of sprayed polyurea elastomer technology in offshore concrete protection," *Painting Guide*, vol. 2, no. 2, p. 5, 2010.
- [33] W. Wang, *Research on the Application of spray Polyurea Technology in the protection of Underground concrete Structures*, Qingdao Technological University, Qingdao, China, 2004.